Accepted Manuscript

A redox-modulated fluorescent strategy for the highly sensitive detection of metabolites by using graphene quantum dots

Hua Liu, Xing Li, Mengke Wang, Xueqian Chen, Xingguang Su

PII: S0003-2670(17)30835-8

DOI: 10.1016/j.aca.2017.07.031

Reference: ACA 235333

To appear in: *Analytica Chimica Acta*

Received Date: 21 April 2017

Revised Date: 9 July 2017

Accepted Date: 11 July 2017

Please cite this article as: H. Liu, X. Li, M. Wang, X. Chen, X. Su, A redox-modulated fluorescent strategy for the highly sensitive detection of metabolites by using graphene quantum dots, *Analytica Chimica Acta* (2017), doi: 10.1016/j.aca.2017.07.031.

A redox-modulated fluorescent strategy for the highly sensitive detection of metabolites by using graphene quantum dots

Hua Liu, Xing Li, Mengke Wang, Xueqian Chen and Xingguang Su*

Department of Analytical Chemistry, College of Chemistry, Jilin University, Changchun 130012, P.R. China

*Corresponding author: Xingguang Su

Tel.: +86-431-85168352

E-mail address: suxg@jlu.edu.cn

ABSTRACT

In this paper, a redox-modulated fluorescent strategy based on the transformation of Fe^{2+}/Fe^{3+} couple and enzymatic reaction for rapid monitoring glucose and uric acid using graphene quantum dots (GQDs) as fluorescent probe was developed. Hydrogen peroxide (H_2O_2) can be produced by the enzymatic reaction of a series of metabolites, such as glucose and uric acid. In the presence of hydrogen peroxide, Fe^{2+} can be oxidized and converted to Fe^{3+}, which have a significant quenching difference in the fluorescence of graphene quantum dots (GQDs). Thus, a sensitive and label-free biosensor for the detection of uric acid and glucose was developed. Under the optimized experimental conditions, the fluorescence intensity was linearly correlated with the concentration of uric acid and glucose in the range of 0.1-45 $\mu molL^{-1}$ and 0.1-30 $\mu molL^{-1}$ with a detection limit of 0.026 $\mu molL^{-1}$and 0.021 $\mu molL^{-1}$, respectively. The proposed method was applied to the determination of uric acid and glucose in human serum samples with satisfactory results, which had potential application to detect metabolites associated with H_2O_2 release.

Key words: Graphene quantum dots; Fe^{2+}/Fe^{3+} couple; Metabolites; Uric acid; Glucose

1. Introduction

As an ideal alternative to the conventional fluorescent probes, graphene quantum dots (GQDs) possess several key advantages, such as good solubility, high biocompatibility, resistance to photobleaching, tunable photoluminescence, ease of functionalization [1,2]. Due to their unique electrical and optical properties, GQDs have attracted great interest in both biomolecule detection [3-5] and biological imaging [1,6,7]. Kim and co-workers investigated the in vitro and in vivo live imaging and tracking of human adipose-derived stem cells using multiphoton luminescent GQDs [8]. Yan et al. illustrated ultrasensitive determination of dopamine in the range of 0.02-105 $\mu molL^{-1}$ based on GQDs-TiO_2 nanocomposites [9]. Poon's group developed a highly sensitive and selective fluorescent sensor for direct trypsin detection in urine using modified GQDs [10].

Quantitative determination of metabolites in blood or other biological samples is important in diagnosis and healthcare. The content of metabolites in blood plays a highly important role in monitoring human disease [2,11]. Abnormal levels of metabolites in blood can cause a variety of diseases. Specifically, Uric acid, 2,6,8-trihydroxypurine, is the main product of purine metabolism [12]. The reference ranges of uric acid in the general population are 0.13-0.46 $mmolL^{-1}$ in serum and 2.49-4.46 $mmolL^{-1}$ in urine [13,14]. Elevated levels of uric acid in blood are signals of high blood pressure, high cholesterol, gout, kidney disease, cardiovascular diseases and so on [15,16]. In contrast, lower uric acid levels are often accompanied by multiple sclerosis and oxidative stress [17,18]. In addition, glucose level in blood is also a key diagnostic parameter for many metabolic disorders such as diabetes mellitus [19,20]. Therefore, it is necessary to develop a rapid, sensitive, accurate and low-cost determination method to monitor the metabolites level in blood.

Current detection assays including electrochemical [20,21], liquid chromatography [22,23] and

mass spectrometry [24] methods have been developed for the detection of uric acid and glucose. However, there are some disadvantages existing in these methods, such as the requirement for complex synthesis or complicated extraction, sophisticated instrumentation, time-consuming, and cumbersome, which limits their practical applications. Compared with the existing other methods, the advantage of fluorescence approach lies in its high sensitivity, rapid response and operational simplicity [25,26]. The application of fluorescent probes, such as carbon nanodots, gold nanoparticles and CdTe nanoparticles, has attracted increasing attention and has been intensively investigated in the detection of metabolites. For example, Ma and co-workers designed a glucose oxidase (GOx)-mediated strategy for glucose detection based on carbon nanodots supported on silver nanoparticles [27]. Liu et al. demonstrated the detection of uric acid based on the inner filter effect of hydrogen peroxide-mediated enlargement of gold nanoparticles using gold nanoclusters as switch-off fluorescent probe [25]. Jin's group developed a method for sensing uric acid based on H_2O_2-induced fluorescence quenching of CdTe nanoparticles [16].

Studies have shown that although both of Fe^{2+} and Fe^{3+}, known as electron acceptor, can rapidly quench the fluorescence of semiconductor quantum dots by electron transfer, Fe^{2+} and Fe^{3+} have different quenching effects on semiconductor quantum dots [28,29]. On the basis of the discrimination of various types of iron, we developed a redox-modulated fluorescent strategy for uric acid and glucose sensing by using GQDs (Scheme1). In the presence of the corresponding enzyme, uric acid and glucose can generate H_2O_2, which can achieve the transformation from Fe^{2+} to Fe^{3+}, leading to more significant fluorescence quenching of GQDs. Thus, a sensitive and label-free biosensor for the detection of uric acid and glucose can be developed.

Scheme 1

2. Experimental section

2.1 Materials

Uric acid and uricase (4.41 U/mg) were purchased from Sangon Biotech (Shanghai) Co. Ltd. H_2O_2 (30 %), H_2SO_4 (98 %), HNO_3 (65 %), glucose, arginine, alanine, glutamic acid, aspartic acid, glycine, cysteine, ascorbic acid were obtained from Beijing Dingguo Biotechnology Co. Ltd. $FeCl_2$, $FeCl_3$, NaCl, KCl and glucose oxidase (GOx) were purchased from Huacheng Biological Co., Ltd (Changchun). All chemicals used were at least of analytical reagent grade and used without further purification. The water used in all experiments had a resistivity higher than 18 $M\Omega \cdot cm^{-1}$.

2.2 Apparatus

All fluorescence spectra were measured by a Shimadzu RF-5301 spectrometer (Shimadzu Co., Kyoto, Japan) using a 1 cm path length quartz cuvette. UV-vis absorption spectra was obtained with a Varian GBC Cintra 10e UV-visible Spectrophotometer. FT-IR spectra was recorded with a Bruker IFS66V FT-IR spectrometer equipped with a DGTS detector (32 scans). All pH measurements were performed on a PHS-3C pH meter (Tuopu Co., Hangzhou, China). All the optical measurements were obtained at room temperature under ambient conditions.

2.3 Synthesis of GQDs

According to a modified Hummer's method, GQDs were prepared from graphite oxide which had been implemented in our previous work [30]. In brief, 0.1 g graphene oxide was weighed into a round bottom flask followed by 20 mL H_2SO_4 and 7 mL HNO_3. The mixture was sonicated for 2

h after stirred for 5 minutes. Afterwards, the mixture was heated to reflux under continuous stirred for 24 h at 80 □ and the color of the mixture gradually changed from black to bright yellow. After cooling down, 50 mL water was slowly added to the solution. Then the solution was further dialyzed through dialysis membrane with a molecular weight cutoff of 3500 Da for 1 day until the pH of the mixture became neutral and the resulting GQDs were stored in 4 □.

2.4 Procedure for uric acid and glucose determination

For the detection of uric acid, the uricase solution (15 μgmL^{-1}) and different concentrations of uric acid were added to a series of 2.0 mL calibrated test tubes followed by the addition of Tris-HCl buffer solution (10 $mmolL^{-1}$, pH 7.4), then the mixture was incubated for 1h at room temperature. Subsequently, Fe^{2+} (120 $\mu molL^{-1}$) and 200 μL GQDs were added, successively. The resulting solution was shaken thoroughly for 20 min at room temperature before fluorescent measurement. GOx solution (7.5 μgmL^{-1}) and Tris-HCl buffer solution (10 $mmolL^{-1}$, pH 6.6) were used in the detection of glucose, and the operation was consistent with the above method for detecting uric acid. The fluorescence spectra were recorded in the 495-750 nm emission wavelength range at the excitation wavelength of 475 nm, the slit width of emission and excitation were both set at 10 nm.

2.5 Real sample assay

Healthy blood samples were supplied by the Hospital of Changchun China, Japan Union Hospital. In order to remove protein in blood samples, acetonitrile was added to the blood samples (the ratio of acetonitrile and blood volume was 1.5: 1) and then the product was centrifuged at 10000 rpm for 10 min after shaking for 2 minutes. The supernatant was stored in -20 □ until testing. The human serum was diluted 50 times and 1000 times with deionized water and a certain

concentration of uric acid and glucose was added to prepare spiked samples, respectively. The detection procedure of real sample followed the method described above. All experiments were performed in compliance with the relevant laws and institutional guidelines, and the writing of informed consent for all samples was obtained from human subjects.

3. Results and discussion

3.1 Characterization of GQDs

The GQDs used in this work was characterized using FT-IR, UV-vis and fluorescence spectrum, which were showed in Fig. S1. As shown in Fig. S1A, the majority characteristic peaks of GQDs could be clearly found through the characteristic peaks of the -OH stretching mode (3446 cm^{-1}), the C=O stretching peak (1732 cm^{-1}), the C=C peak (1635 cm^{-1}) and C-O-C (1170 cm^{-1}), which was consistent with the previous work [30,31]. The UV-vis absorption spectra and the fluorescence emission spectra of GQDs were showed in Fig. S1B. It could be seen that the fluorescence emission of GQDs at 535 nm was maximum when excited at 475 nm, so the excitation wavelength of 475 nm was used in further experiment. Furthermore, the strong absorbance at 230 nm and weak shoulder peak at around 300 nm, which maybe result from π–π* transition of aromatic structures and n-π* transition of C=O, respectively [32,33], shown in the UV-vis absorption spectra of GQDs further demonstrated the formation of GQDs.

3.2 The design strategy for uric acid and glucose detection

According to the previous reports, compared to Fe^{2+}, Fe^{3+} can quench the fluorescence of semiconductor quantum dots more significantly [28,29], and H_2O_2 can be generated by the enzymatic reaction of uric acid or glucose [16,27]. Namely, the fluorescence of GQDs can be further quenched in the GQDs/Fe^{2+}/enzyme system with the addition of uric acid or glucose. In

order to prove the feasibility of the strategy, the effect of different components on the fluorescence intensity of GQDs was studied. As shown in Fig. 1, H_2O_2 was not able to result in considerable fluorescence quenching of GQDs and Fe^{2+} could slightly quench the fluorescence of GQDs, while the fluorescence intensity of GQDs could be dramatically decreased by Fe^{3+} or the mixture of H_2O_2 and Fe^{2+}. Moreover, there is no significant change of the fluorescence intensity of the GQDs/Fe^{2+} system after mixed with uric acid, glucose, uricase or GOx separately. As expected, uric acid/uricase and glucose/GOx can achieve almost the same effect as H_2O_2 on the fluorescence of GQDs/Fe^{2+} system. It is consistent with the mechanism illustrated in Scheme 1, and further proves that glucose and uric acid in the presence of GOx and uricase, respectively, can product H_2O_2, and H_2O_2 could oxidize Fe^{2+} to Fe^{3+}, which can dramatically decrease the fluorescence intensity of GQDs.

Fig. 1

3.3 Optimization for uric acid and glucose detection

In order to optimize the sensing conditions for uric acid and glucose detection, we optimized the incubation time, pH and the concentration of Fe^{2+}, uricase and GOx. In this work, the concentration of Fe^{2+} and the incubation time of H_2O_2 were investigated firstly. As shown in Fig. 2A, the fluorescence intensity of the GQDs decreased gradually with the increase of the concentration of Fe^{2+} and Fe^{3+}, and the difference of the fluorescence quenching effect between Fe^{2+} and Fe^{3+} increased gradually with increasing the concentration of Fe^{2+} and Fe^{3+} and then kept constant when the concentration of Fe^{2+} and Fe^{3+} is more than 120 $\mu molL^{-1}$. According to Fig. 2B,

it can be observed that the fluorescence intensity of GQDs/Fe^{2+}/H_2O_2 system decreased rapidly in the first 10 min, then kept constant after 20 min. Thus 120 μmolL^{-1} Fe^{2+} and the incubation time of 20 min was chosen in the further experiments.

Fig. 2

Prior to the addition of Fe^{2+} and GQDs, the incubation of metabolite and enzyme is necessary. The effect of incubation time, pH and the concentration of enzyme on uric acid and glucose detection were investigated in the Fig. 3. According to Fig. 3A-B, it can be observed that the fluorescence intensity of GQDs/Fe^{2+}/enzyme/uric acid or glucose system decrease with the increasing incubation time of uric acid and uricase or glucose and GOx, and then remained stable after 60 minutes. So 60 minutes was chosen as the incubation time for uric acid and uricase or glucose and GOx. The effect of pH on the fluorescence intensity of the sensing system was showed in the Fig. 3C-D. As shown in Fig. 3C, the fluorescence intensity of GQDs and GQDs/Fe^{2+} system in the pH range of 5.8-7.4 were stable and the difference of the fluorescence intensity between GQDs/Fe^{2+} and GQDs/Fe^{2+}/uricase/uric acid system was the largest at pH 7.4. From Fig. 3D, it can be seen that the fluorescence intensity of GQDs/Fe^{2+}/GOx/glucose system were the lowest in the pH range of 5.8-7.0, which demonstrates that alkaline conditions are not suitable for the enzymatic reaction of glucose and GOx. Thus pH 7.4 and pH 6.6 were adopted for uric acid and glucose detection in the further experiments, respectively. Moreover, the effect of the concentration of uricase and GOx on the fluorescence intensity of the sensing system were showed in the Fig. 3E-F. As shown in Fig. 3E-F, the fluorescence intensity of the sensing system, at first,

dropped rapidly with the increase of uricase and GOx concentration, and then remained stable when the concentration of uricase and GOx were more than 15 μgmL^{-1} and 7.5 μgmL^{-1}, respectively. So we selected 15 μgmL^{-1} uricase and 7.5 μgmL^{-1} GOx as the concentration of the enzyme in the further experiments.

Fig. 3

3.4 Detection of uric acid and glucose

The fluorescence emission spectra of GQDs/Fe^{2+}/uricase system with different concentrations of uric acid were shown in Fig. 4. It can be seen from Fig. 4 that the fluorescence intensity of GQDs/Fe^{2+}/uricase system was gradually decreased with the increase of uric acid concentration. And Fig. 4 inset showed there was a good linear relationship between $(I-I_0)/I_0$ (I_0 and I were the fluorescence intensity of GQDs/Fe^{2+}/uricase system in the absence and presence of uric acid, respectively) and the concentration of uric acid in the range of 0.1-45 $\mu molL^{-1}$. The linear regression equation was $(I_0-I)/I_0$ = 0.00143 + 0.01063 [uric acid], $\mu molL^{-1}$, with a correlation coefficient R^2 = 0.9972, and the detection limit is 0.026 $\mu molL^{-1}$. The detection limit was defined by the equation LOD=3σ/s, where σ is the standard deviation of the corrected blank signals and s is the slope of the calibration curve.

Fig. 4

As shown in Fig. 5, the fluorescence intensity of GQDs/Fe^{2+}/GOx system was gradually

decreased with the increase of glucose concentration under the optimized experimental conditions, Fig. 5 inset showed there was a good linear relationship between $(I-I_0)/I_0$ (I_0 and I were the fluorescence intensity of GQDs/Fe^{2+}/GOx system in the absence and presence of glucose, respectively) and the concentration of glucose in the range of 0.1-30 $\mu molL^{-1}$. The regression equation of glucose is $(I_0-I)/I_0$ = 0.00328 + 0.01313 [glucose], $\mu molL^{-1}$, the corresponding regression coefficient (R^2) is 0.9973, and the detection limit is 0.021 $\mu molL^{-1}$.

Fig. 5

A comparison of materials, linear ranges and detection limits between the present method and some other methods for uric acid and glucose determination reported previously was listed in Table 1 and Table 2. Compared with other methods, the method we established is more environmentally friendly and sensitive.

Table 1

Table 2

3.5 Interference study

To evaluate the selectivity of the present method for the uric acid and glucose detection, we studied the influences of various common coexisting substances in human serum on the fluorescence of GQDs/Fe^{2+}/enzyme and GQDs/Fe^{2+}/enzyme/uric acid or glucose system,

including NaCl, KCl, arginine, alanine, glutamic acid, aspartic acid, glycine, cysteine, glucose, uric acid, ascorbic acid. As shown in Fig. 6, common metal ions and biomolecules had little effect on the fluorescence of GQDs/Fe^{2+}/enzyme and GQDs/Fe^{2+}/enzyme/uric acid or glucose system, which was considered to be tolerable. The results showed that common metal ions and biomolecules had no obvious interference on the detection of uric acid and glucose, indicating that this method had a high selectivity toward uric acid and glucose.

Fig. 6

3.6 Real samples detection

In order to evaluate the applicability of the proposed method, we detected uric acid and glucose in human serum samples. The results obtained by the standard addition method were shown in Table S1 and Table S2. It can be observed that the average recovery of uric acid and glucose were in the range of 97.6%-102.9% and 98.0%-103.3%, respectively, and the relative standard deviation (RSD) were both lower than 3.5%. The above results demonstrated that the proposed method has potential application in real sample detection of uric acid and glucose.

4. Conclusion

In conclusion, a facile and sensitive method for the detection of uric acid and glucose was developed based on the difference abilities of the fluorescence quenching between Fe^{2+} and Fe^{3+} and enzymatic reaction. Under the optimum condition, a good linear response for uric acid and glucose was found in the range of 0.1-45 $\mu molL^{-1}$ and 0.1-30 $\mu molL^{-1}$, with a detection limit of

0.026μmolL^{-1} and 0.021 μmolL^{-1}, respectively. The method was successfully applied in real sample detection with satisfactory results and good repeatability. In comparison with the previous reports, the proposed method is simple, low cost and has a higher sensitivity and specificity.

Acknowledgments

This work was finally supported by the National Natural Science Foundation of China (No. 21075050 and No. 21275063), the Science and Technology Development project of Jilin province, China (No. 20150204010GX).

References

[1] X.T. Zheng, A. Than, A. Ananthanaraya, D.-H. Kim, P. Chen, ACS nano, 7 (2013) 6278.

[2] N. Li, A. Than, X. Wang, S. Xu, L. Sun, H. Duan, C. Xu, P. Chen, ACS nano, 10 (2016) 3622.

[3] Z. Liu, J. Xiao, X. Wu, L. Lin, S. Weng, M. Chen, X. Cai, X. Lin, Sensors and Actuators B-Chemical, 229 (2016) 217.

[4] S. Huang, L. Wang, F. Zhu, W. Su, J. Sheng, C. Huang, Q. Xiao, Rsc Advances, 5 (2015) 44587.

[5] J. Liu, Z. Liu, C.J. Barrow, W. Yang, Anal. Chim. Acta, 859 (2015) 1.

[6] J. Shen, Y. Zhu, X. Yang, C. Li, Chem. Commun., 48 (2012) 3686.

[7] J. Wen, Y. Xu, H. Li, A. Lu, S. Sun, Chem. Commun., 51 (2015) 11346.

[8] H. Sun, N. Gao, K. Dong, J. Ren, X. Qu, ACS nano, 8 (2014) 6202.

[9] Y. Yan, Q. Liu, X. Du, J. Qian, H. Mao, K. Wang, Anal. Chim. Acta, 853 (2015) 258.

[10] C.-Y. Poon, Q. Li, J. Zhang, Z. Li, C. Dong, A.W.-M. Lee, W.-H. Chan, H.-W. Li, Anal. Chim. Acta, 917 (2016) 64.

[11] W. Gu, S. Gong, Y. Zhou, Y. Xia, Biosens. Bioelectron., 90 (2017) 487.

[12] A. Fang, Q. Wu, Q. Lu, H. Chen, H. Li, M. Liu, Y. Zhang, S. Yao, Biosens. Bioelectron., 86 (2016) 664.

[13] P. Kanyong, R.M. Pemberton, S.K. Jackson, J.P. Hart, Anal. Biochem., 428 (2012) 39.

[14] N. Chauhan, C.S. Pundir, Anal. Biochem., 413 (2011) 97.

[15] Q. Long, A. Fang, Y. Wen, H. Li, Y. Zhang, S. Yao, Biosens. Bioelectron., 86 (2016) 109.

[16] D. Jin, M.-H. Seo, H. Bui The, P. Quoc-Thai, M.L. Conte, D. Thangadurai, Y.-I. Lee, Biosens. Bioelectron., 77 (2016) 359.

[17] T. Ghosh, P. Sarkar, A.P.F. Turner, Bioelectrochemistry, 102 (2015) 1.

[18] N. Misra, V. Kumar, L. Borde, L. Varshney, Sensors and Actuators B-Chemical, 178 (2013) 371.

[19] P. Salazar, V. Rico, A.R. Gonzalez-Elipe, Sensors and Actuators B-Chemical, 226 (2016) 436.

[20] A. Zhao, Z. Zhang, P. Zhang, S. Xiao, L. Wang, Y. Dong, H. Yuan, P. Li, Y. Sun, X. Jiang, F. Xiao, Anal. Chim. Acta, 938 (2016) 63.

[21] X. Zhang, Y.-C. Zhang, L.-X. Ma, Sensors and Actuators B-Chemical, 227 (2016) 488.

[22] X.L. Li, G. Li, Y.Z. Jiang, D.Z. Kang, C.H. Jin, Q. Shi, T.F. Jin, K. Inoue, K. Todoroki, T. Toyo'oka, J.Z. Min, Journal of Chromatography B-Analytical Technologies in the Biomedical and Life Sciences, 1002 (2015) 394.

[23] Z.L. Ling, P. Xu, Z.Y. Zhong, F. Wang, N. Shu, J. Zhang, X.G. Tang, L. Liu, X.D. Liu, Biomed. Chromatogr., 30 (2016) 601.

[24] S.M. Chen, H.Z. Zheng, J.N. Wang, J. Hou, Q. He, H.H. Liu, C.Q. Xiong, X.L. Kong, Z.X. Nie, Analytical Chemistry, 85 (2013) 6646.

[25] Y. Liu, H. Li, B. Guo, L. Wei, B. Chen, Y. Zhang, Biosens. Bioelectron., 91 (2017) 734.

[26] S. Li, Y. Li, J. Cao, J. Zhu, L. Fan, X. Li, Analytical Chemistry, 86 (2014) 10201.

[27] J.-L. Ma, B.-C. Yin, X. Wu, B.-C. Ye, Analytical Chemistry, 89 (2017) 1323.

[28] Q. Ma, Y. Li, Z.-H. Lin, G. Tang, X.-G. Su, Nanoscale, 5 (2013) 9726.

[29] N. Li, A. Than, C. Sun, J. Tian, J. Chen, K. Pu, X. Dong, P. Chen, ACS nano, 10 (2016) 11475.

[30] Y. Li, N. Cai, M. Wang, W. Na, F. Shi, X. Su, Rsc Advances, 6 (2016) 33197.

[31] J. Peng, W. Gao, B.K. Gupta, Z. Liu, R. Romero-Aburto, L. Ge, L. Song, L.B. Alemany, X. Zhan, G. Gao, S.A. Vithayathil, B.A. Kaipparettu, A.A. Marti, T. Hayashi, J.-J. Zhu, P.M. Ajayan, Nano Lett., 12 (2012) 844.

[32] K.S. Novoselov, A.K. Geim, S.V. Morozov, D. Jiang, Y. Zhang, S.V. Dubonos, I.V. Grigorieva, A.A. Firsov, Science, 306 (2004) 666.

[33] Y.X. Fang, S.J. Guo, D. Li, C.Z. Zhu, W. Ren, S.J. Dong, E.K. Wang, ACS nano, 6 (2012) 400.

[34] Z.-H. Sheng, X.-Q. Zheng, J.-Y. Xu, W.-J. Bao, F.-B. Wang, X.-H. Xia, Biosens. Bioelectron., 34 (2012) 125.

[35] H. Lu, J. Li, M. Zhang, D. Wu and Q. Zhang, Sensors and Actuators B-Chemical, 244 (2017) 73.

[36] J. Pal, T. Pal, Rsc Advances, 6 (2016) 83738.

[37] J. Yang, M. Cho, Y. Lee, Biosens. Bioelectron., 75 (2016) 15.

[38] L. Han, C. Shao, B. Liang, A. Liu, ACS applied materials & interfaces, 8 (2016) 13768.

[39] S. Chen, X. Hai, X.-W. Chen, J.-H. Wang, Analytical Chemistry, 86 (2014) 6689.

[40] L. Jin, Z. Meng, Y. Zhang, S. Cai, Z. Zhang, C. Li, L. Shang, Y. Shen, ACS applied materials & interfaces, 9 (2017) 10027.

[41] Z. Song, R.T.K. Kwok, D. Ding, H. Nie, J.W.Y. Lam, B. Liu, B.Z. Tang, Chem. Commun., 52 (2016) 10076.

Captions:

Scheme 1 Schematic illustration of the sensing process for uric acid and glucose.

Fig. 1. The fluorescence spectra of GQDs under different conditions. Concentration: 120 $\mu molL^{-1}$ Fe^{2+}, 100 $\mu molL^{-1}$ H_2O_2, 15 μgmL^{-1} uricase, 100 $\mu molL^{-1}$ uric acid, 7.5 μgmL^{-1} GOx, 100 $\mu molL^{-1}$ glucose.

Fig. 2. The effect of (A) the concentration of Fe^{2+} and Fe^{3+} on the fluorescence intensity of GQDs and (B) incubating time on the fluorescence intensity of GQDs/Fe^{2+}/H_2O_2 system. The concentration of Fe^{2+} and H_2O_2 were 120 $\mu molL^{-1}$ and 100 $\mu molL^{-1}$, respectively.

Fig. 3. The effect of (A, B) incubating time and (C, D) The effect of pH on the fluorescence intensity of the sensing system of glucose and uric acid, respectively. The effect of the concentration of (E) uricase (0, 5, 10, 15, 20, 25, 30, 35, 40, 45, 50 μgmL^{-1}, respectively) and (F) GOx (0, 1.0, 2.5, 5.0, 7.5, 10, 12.5, 15 μgmL^{-1}, respectively) on the fluorescence intensity of the sensing system of uric acid and glucose, respectively.

Fig. 4. (A) The fluorescence emission spectra of GQDs/Fe^{2+}/uricase system with different concentrations of uric acid in the range of 0-100 $\mu molL^{-1}$ (0, 0.1, 0.4, 0.7, 1, 2, 4, 6, 8, 10, 15, 20, 25, 30, 35, 40, 45, 50, 60, 70, 80, 90, 100 $\mu molL^{-1}$). (B) The relationship between quenching efficiency ($(I_0-I)/I_0$) and uric acid concentration. The error bars (RSD) were gained from three parallel test results. Concentration: 120 $\mu molL^{-1}$ Fe^{2+}, 15 μgmL^{-1} uricase.

Fig. 5. (A) The fluorescence emission spectra of GQDs/Fe^{2+}/GOx system with different concentrations of glucose in the range of 0-100 $\mu molL^{-1}$ (0, 0.1, 1, 2, 4, 6, 8, 10, 15, 20, 25, 30, 35, 40, 45, 50, 55, 60, 70, 80, 90, 100 $\mu molL^{-1}$). (B) The relationship between quenching efficiency ($(I_0-I)/I_0$) and glucose concentration. The error bars (RSD) were gained from three parallel test

results. Concentration: 120 μmolL^{-1} Fe^{2+}, 7.5 μgmL^{-1} GOx.

Fig. 6. The selectivity of the GQDs/Fe^{2+} system for detection of (A) uric acid (50 μmolL^{-1}) and (B) glucose (50 μmolL^{-1}) over coexisting substances: 1000 μmolL^{-1} NaCl, 1000 μmolL^{-1} KCl, 250 μmolL^{-1} arginine, 250 μmolL^{-1} alanine, 250 μmolL^{-1} glutamic acid, 250 μmolL^{-1} aspartic acid, 250 μmolL^{-1} glycine, 50 μmolL^{-1} cysteine, 500 μmolL^{-1} glucose, 50 μmolL^{-1} uric acid, 25 μmolL^{-1} ascorbic acid.

Table 1 Comparison of different methods for the determination of uric acid

Table 2 Comparison of different methods for the determination of glucose

1 **Figures:**

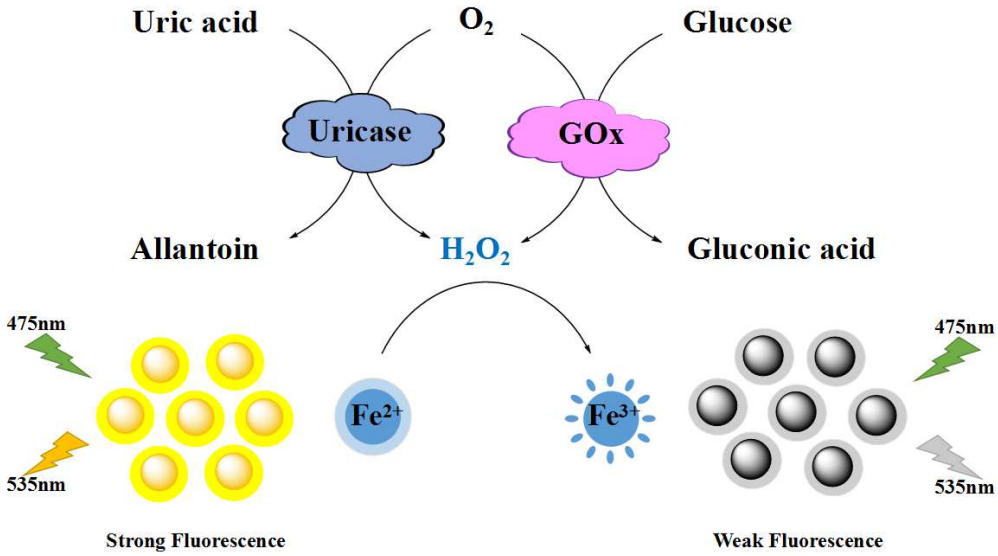

2

3 **Scheme 1**

4

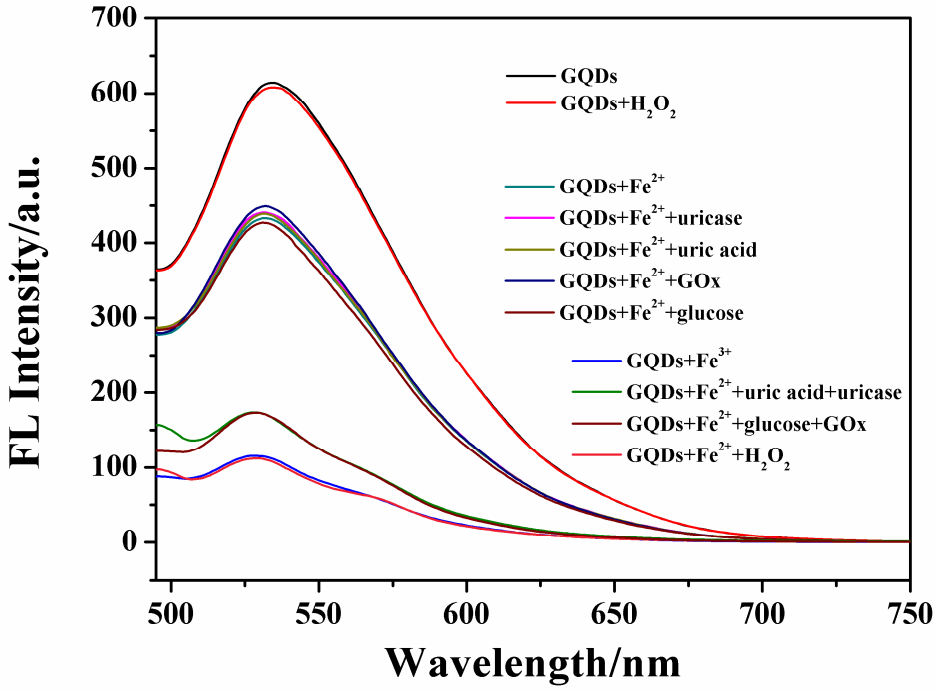

Fig. 1

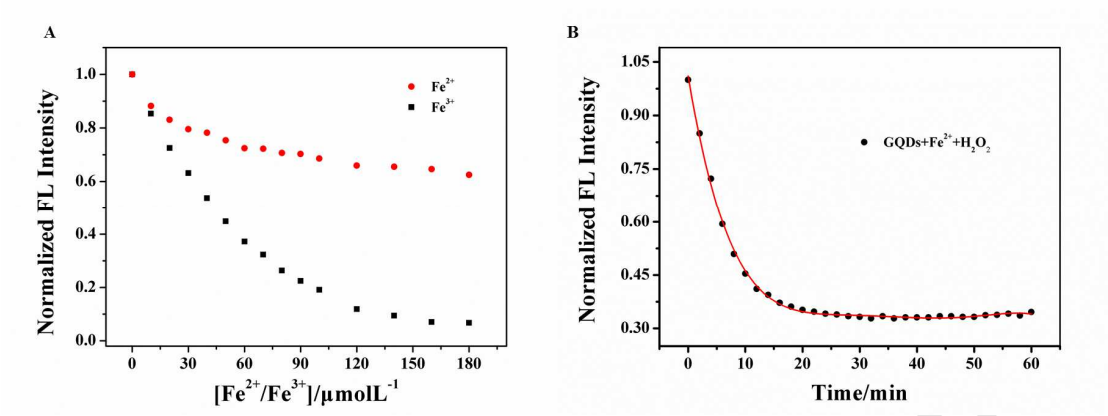

Fig. 2

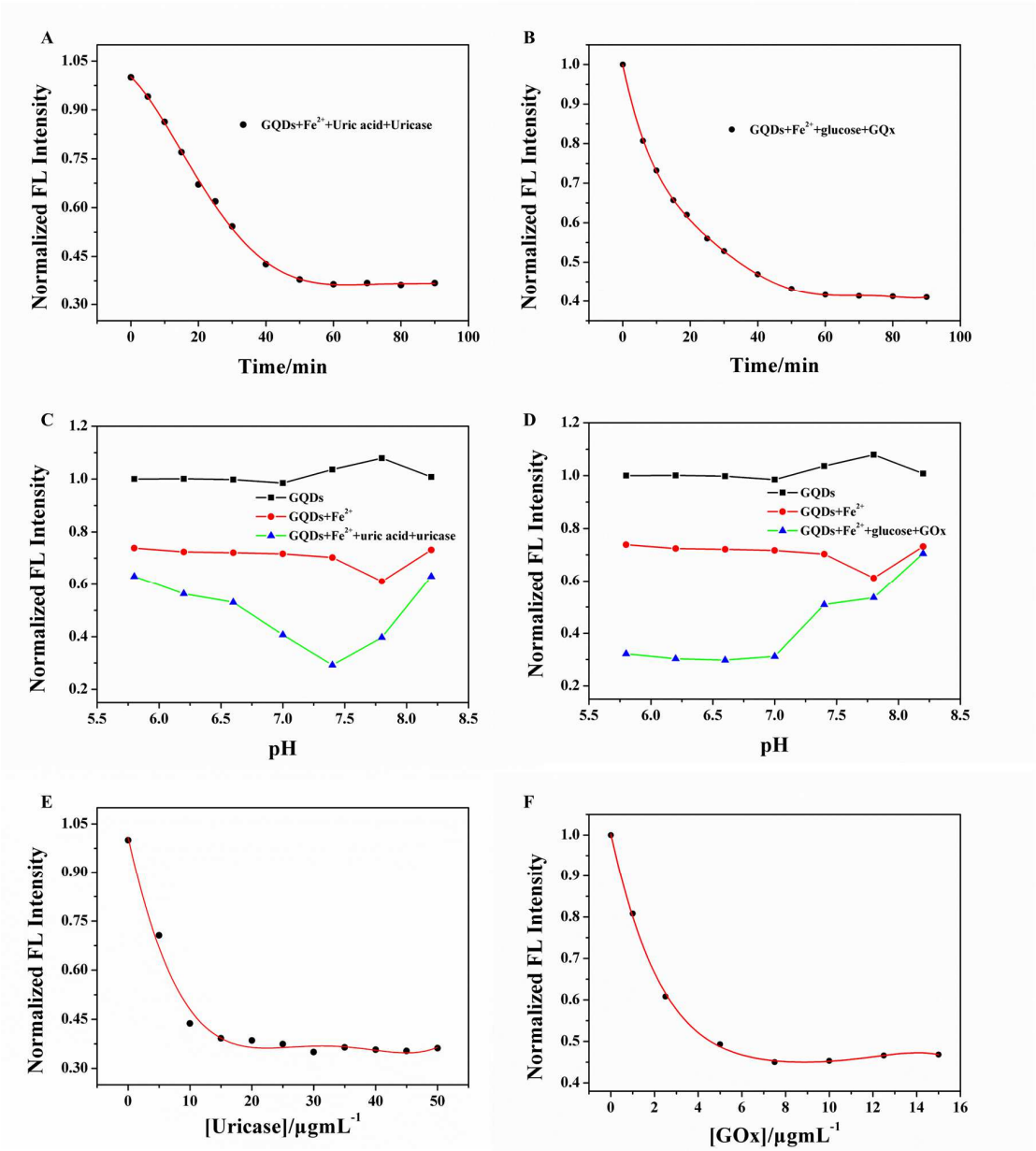
A
Normalized FL Intensity
GQDs+Fe2+ +Uric acid+Uricase
Time/min
B
Normalized FL Intensity
GQDs+Fe2+ +glucose+GQx
Time/min
C
Normalized FL Intensity
GQDs
GQDs+Fe2+
GQDs+Fe2+ +uric acid+uricase
pH
D
Normalized FL Intensity
GQDs
GQDs+Fe2+
GQDs+Fe2+ +glucose+GOx
pH
E
Normalized FL Intensity
[Uricase]/μgmL-1
F
Normalized FL Intensity
[GOx]/μgmL-1

Fig. 3

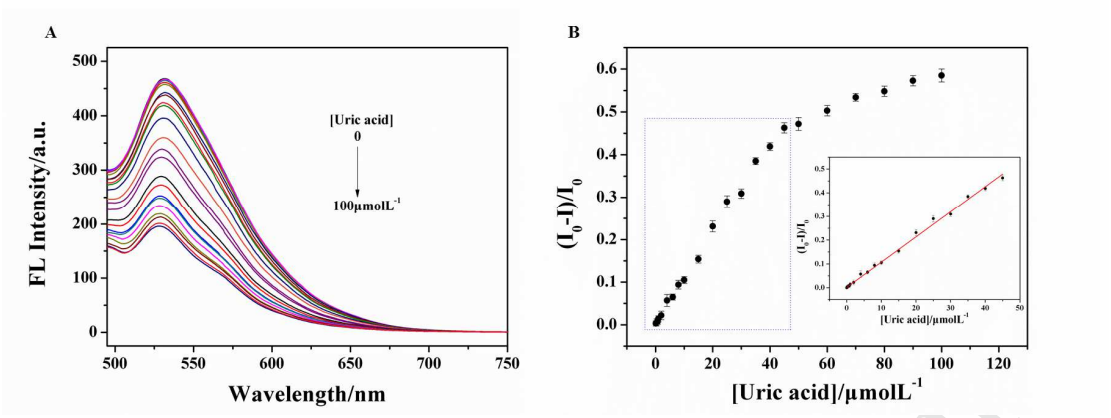

Fig. 4

1

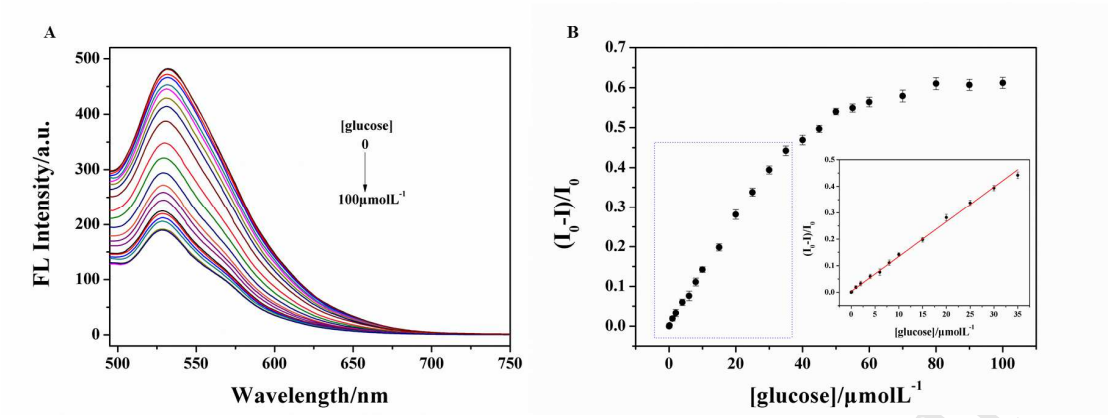

2 **Fig. 5**

3

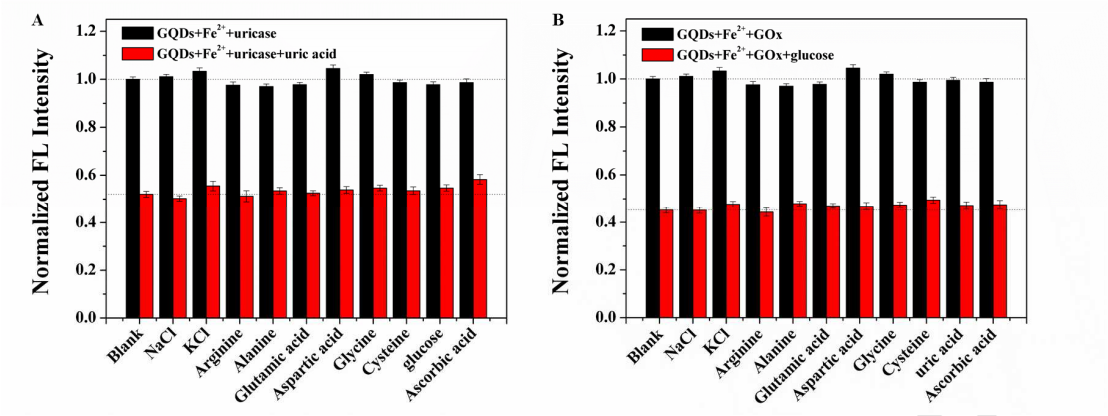

Fig. 6

1 **Table 1** Comparison of different methods for the determination of uric acid

Methods	Materials	Linear range ($\mu molL^{-1}$)	Detection limit ($\mu molL^{-1}$)	Reference
Electrochemical	graphene-zinc oxide composite	1-70	0.33	[21]
Electrochemical	Nitrogen doped graphene	0.1-20	0.045	[34]
Colorimetric	TMB/Cu^{2+}/uricase	1-100	0.64	[35]
Colorimetric	TMB/Ni@MnO_2	1-40	0.24	[36]
Fluorescence	Gold nanoclusters	5-100	1.7	[25]
Fluorescence	CdTe nanoparticles	0.22-6	0.1	[16]
Fluorescence	GQDs	0.1-45	0.026	This work

2

3

1 **Table 2** Comparison of different methods for the determination of glucose

Methods	Materials	Linear range ($\mu molL^{-1}$)	Detection limit ($\mu molL^{-1}$)	Reference
Electrochemical	Hierarchical $NiCo_2O_4$ hollow nanorods	0.3-1000	0.16	[37]
Electrochemical	Phage-Templated MnO_2 Nanowires	5-2000	1.8	[38]
Colorimetric	AgNPs@GQDs	0.5-400	0.17	[39]
Colorimetric	Pt nanoclusters	0-400	0.28	[40]
Fluorescence	Tetraphenylethene derivative	0-200	-	[41]
Fluorescence	C-dots/AgNPs	2-100	1.39	[27]
Fluorescence	GQDs	0.1-30	0.021	This work

2

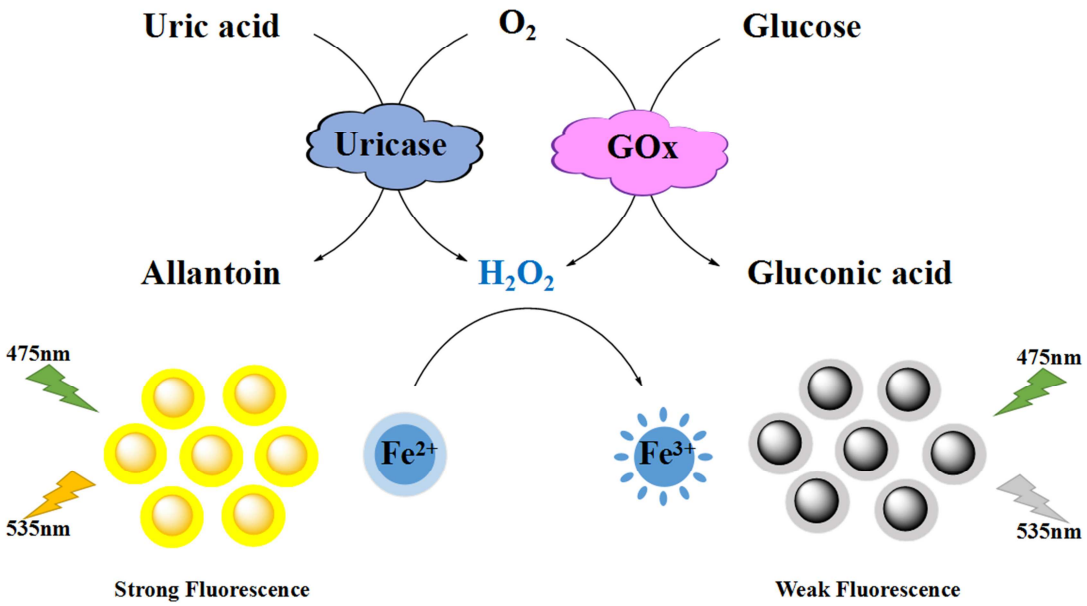

Highlights:

►GQDs with a fluorescence emission peak of 535 nm were used to detect uric acid and glucose.

► The fluorescent strategy is based on the transformation of Fe^{2+}/Fe^{3+} couple and enzymatic reaction.

► The method was simple, low cost and had a higher sensitivity and better selectivity.

► Uric acid and glucose in real samples were detected with satisfactory results.

► The method had potential application to detect metabolites associated with H_2O_2 release.